Available online at www.sciencedirect.com

ScienceDirect

Energy Procedia 92 (2016) 652 – 660

Energy Procedia

6th International Conference on Silicon Photovoltaics, SiliconPV 2016

"Cold" process for IBC c-Si solar cells fabrication

Gema López*, Pablo R. Ortega, Isidro Martín, Cristóbal Voz, Albert Orpella, Ramón Alcubilla

Departament d'Enginyeria Electrònica, Universitat Politècnica de Catalunya, C/Jordi Girona 1-3, Mòdul C4, 08034 Barcelona, Spain

Abstract

In this work we have developed an innovative fabrication process of n-type interdigitated back contact (IBC) c-Silicon solar cells. The main feature is that all the highly-doped regions in the cell have been entirely fabricated through laser processing of dielectric layers, avoiding the high temperature steps typically found in conventional diffusion processes. Additionally, we have reduced the patterning steps. We use an Al_2O_3 film deposited by thermal-ALD that passivates the front and rear surfaces acting simultaneously as antireflection coating and aluminium source for p+ emitter formation. Back surface field (BSF) is achieved by the introduction of phosphorous atoms from a N doped a-SiC_x stack deposited by PECVD. This stack consists of intrinsic a-SiC_x as passivating layer, a-Si (n type) as phosphorous source and a-SiC_x carbon rich as protective capping layer. Dielectrics were laser processed in a point- like structure to achieve highly-doped regions. As a proof of concept we have developed four 9 cm^2-IBC varying the emitter coverage with efficiencies up to 15.5 %. However, our 3D simulations suggest that efficiency beyond 20 % is reachable by future improvements in the laser process stage.

Peer review by the scientific conference committee of SiliconPV 2016 under responsibility of PSE AG.

Keywords: IBC solar cell; Al_2O_3; laser doping

* Corresponding author. Tel.: +34-93-4015671; fax: :+34-93-4016756.
E-mail address: gema.lopez@upc.edu

Peer review by the scientific conference committee of SiliconPV 2016 under responsibility of PSE AG.
doi:10.1016/j.egypro.2016.07.032

1. Introduction

Interdigitated Back-Contact (IBC) back-junction solar cells exhibit the emitter and base electrodes on the rear side of the cell. This structure provides some advantages over double side contacted solar cells. The absence of metal grid at the front eliminates shading losses. Then, front surface requirements are relaxed in terms of electrical contact and only optimum light trapping and surface passivation properties have to be considered. In addition, series resistance due to the metal grid can be reduced because the metal finger width is not limited by its shading and the solar cells interconnection is clearly simplified [1,2]. As a consequence, this solar cell architecture has a great efficiency potential. In fact, the highest conversion efficiency of crystalline solar cell for one-sun applications is 25.6% and was achieved by Panasonic (2014) [3] using back-contact back-junction structure with heterojunction technology. However, IBC solar cell fabrication involves complex patterning steps for the interdigitated rear structure. Furthermore, since both contacts are on the rear side, the fabrication process must ensure low recombination at the surfaces. In this sense, the passivation of front surface is particularly important as well as a good quality substrate with long bulk lifetimes [4,5].

On the other hand, the use of laser processes to create doped regions into crystalline silicon (c-Si) can significantly reduce time and energy consumption in the fabrication process of a c-Si solar cell. Different approaches have been reported using laser beam with different doping sources: phosphosilicate glass grown on c-Si surface during the conventional diffusion [6,7], spin-on dopant [8,9], chemical liquid [10,11] are some examples. Dielectric layers like phosphorus-doped silicon nitride, phosphorus-doped silicon carbide or aluminium oxide have also been used for the creation doped region by means of laser processing [12,13,14].

In the present work, we have developed an IBC solar cell combining dielectric layers as a doping source. The implementation of laser doping technique drastically simplifies the fabrication process reducing the global thermal budget.

2. IBC structure and fabrication

Solar cells were fabricated on n-type float zone (FZ) c-Si wafers. The starting thickness was 275±10 μm and the base resistivity 2.5 ± 0.5 Ωcm. In figure 1 a cross-section of the device structure is depicted. The front side was randomly textured with a tretamethyl ammonium hydroxide (TMAH) solution, while the rear side was protected by thermally grown SiO_2. Then, after removing the SiO_2, the wafer was cleaned following a RCA sequence. Both sides were coated with a 50 nm thick Al_2O_3 layer grown by thermal-ALD. Following, the sample was annealed at 400 ºC for 10 min in H_2/N_2 atmosphere, in order to activate the negative charge in the Al_2O_3/c-Si interface to improve the passivation [15]. Therefore, no front diffusion (no front surface field (FSF)) is considered in this structure due to the low front surface recombination velocity obtained. After that, a 35 nm thick of stoichiometric a-SiC_x layer was deposited on both sides by PECVD. The reason to include a-SiC_x as a capping layer on Al_2O_3 is chemical protection of the Al_2O_3 films during cleaning/etching steps in the IBC fabrication process. Additionally, it has been demonstrated that an a-SiC_x capping also improves the laser contact formation on c-Si solar cells compared to a standard Laser Fired Contact (LFC) process [16,17]. After a photolithographic step, the rear a-SiC_x and Al_2O_3 layers were removed from undesired regions (base regions) with plasma and HF etching respectively. After a RCA cleaning, we deposited on the entire rear side by PECVD a dielectric stack consisting of a Si-rich intrinsic a-SiC_x(x~0.1) passivating layer (~ 4 nm), a doped a-Si layer (~ 15 nm) acting as a phosphorous atom source and a stoichiometric a-SiC_x(x~1) 35 nm thick film.

Back surface field (BSF,n++) and emitter (p++) result from the laser irradiation of these dielectric layers applying a pulsed Nd-YAG 1064 nm laser in the nanosecond regime. Contacts are defined in a point-like structure with 250 μm separation (pitch). Four emitter coverages were defined: one base laser spot per 2, 3, 4 or 6 emitter spots, corresponding to 66, 75, 80 and 85 % emitter coverage respectively. Finally, a metal interdigitated pattern is formed with Ti and Al and defined by photolithographic step and a subsequent Ti and Al wet etching.

The whole process implies no thermal steps beyond 400 ºC. Only one photolithographic step is needed in addition to the metal definition.

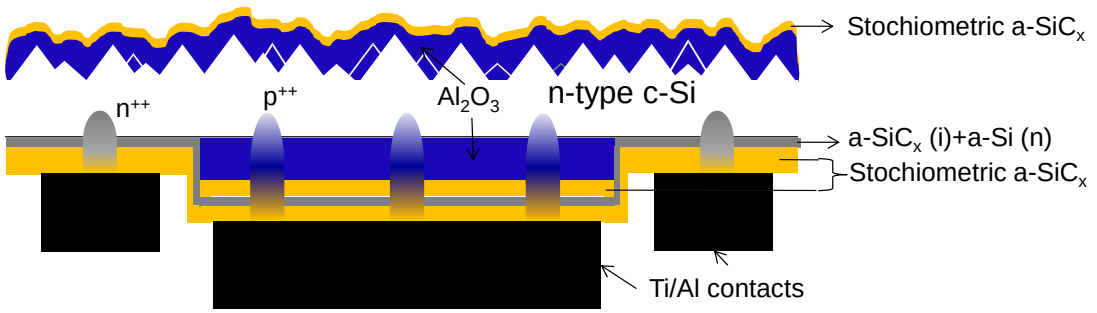

Fig. 1. Cross-section sketch of the proposed n-type IBC structure.

3. Results and discussion

3.1. Surface passivation and optical properties test

Surface passivation quality was determined from effective minority carrier lifetime (τ_{eff}) measurements by quasi-steady-state photoconductance (QSSPC) method using WCT-120 apparatus from Sinton Consulting. On one test sample we emulate the Al_2O_3 passivated surfaces that can be found in the final device by defining, one side randomly textured and both faces symmetrically passivated with 50nm Al_2O_3 and 35 nm of a-SiC_x. Another sample was used to assess the surface passivation provided by the intrinsic Si-rich a-SiC_x film. An upper limit to the surface recombination velocity ($S_{eff,max}$) was estimated in 9.5 cm/s and 13 cm/s respectively, which correspond to one-sun effective lifetimes of 1.4 ms and 1 ms and 5 ms and 1.3 ms maximum respectively (figure 2).

As a rule of thumb, in order to assure a surface passivation and high quality substrate suitable for the fabrication of high-efficiency IBC solar cells, the effective minority diffusion length (L_{eff}) in the bulk must be at least four times greater than the wafer thickness [18]. L_{eff} is related with τ_{eff} by the diffusivity (D) according to:

$$L_{eff} = \sqrt{D.\tau_{eff}}$$

Then, using the τ_{eff} values at 10^{15} cm^{-3} and a hole diffusivity of 11.93 cm^2/s corresponding to n-type FZ c-Si with base resistivity of 2.5 Ωcm L_{eff} is calculated in 2442 µm in the case of the sample with Al_2O_3 and 1245 µm in the case of a-SiC_x sample . Therefore, the surface passivation and the high quality of the c-Si sample guarantee the conditions to the IBC fabrication.

Optical properties were measured by UV-VIS-NIR Spectrophotometry (using anintegrating sphere). The sample under test for reflectance measurements was randomly textured and the surface passivated with 50 nm thick Al_2O_3 and 35 nm thick a-SiC_x stack. Also a borosilicate glass was coated with the same stack for absorbance measurement. The corresponding spectra are shown in figure 3. As it can be observed, reflectance below 1% (from 450 to 1000 nm) is obtained when textured c-Si is coated by the Al_2O_3/a-SiC_x stack. Absorption of light by the Al_2O_3 layer does can be neglected in the relevant wavelength range for photovoltaic applications. The absorbance of the a-SiC_x layer gradually increases from 500 nm to 300 nm up to 13% (inset). Then, a-SiC_x capping film is less convenient to be used as antireflection layer on the illuminated side of the solar cell compared to a single Al_2O_3 film. However, the SiC_x layer is needed for chemical protection of the Al_2O_3 films in subsequent cleaning/etching steps during the fabrication process.

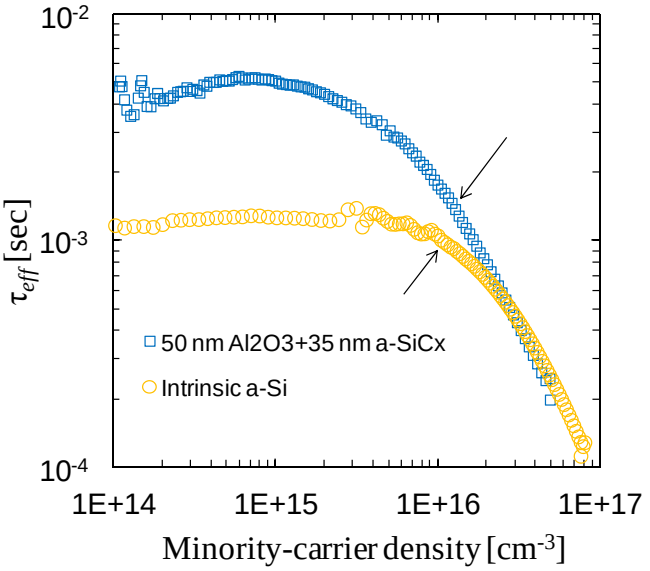

Fig. 2. τ_{eff} as a function of minority-carrier density. Arrows show the values for 1 sun injection level.

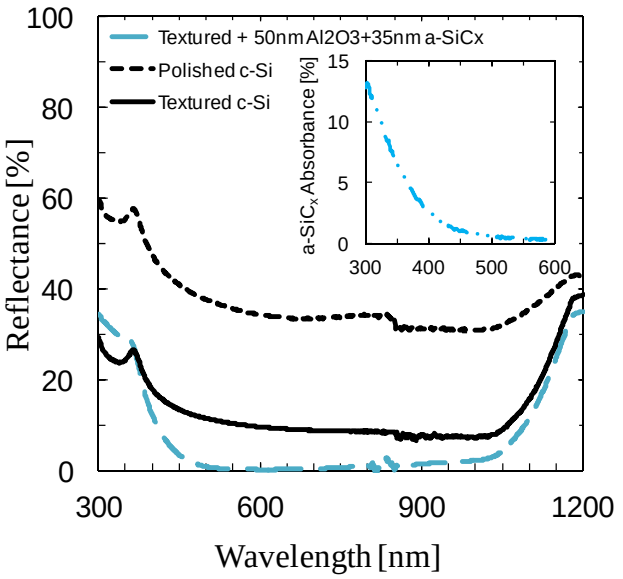

Fig. 3. Reflectance of textured c-Si coated by 50 nm thick Al_2O_3 and 35 nm a-SiC_x thick (long dashed blue line). Textured c-Si (black line) and bare polished c-Si (short dashed black line) is shown as a reference. Inset shows the absorbance of the 50 nm Al_2O_3 and 35 nm a-SiC_x stack.

3.2. Optimal power laser conditions test

Power laser conditions for creating the emitter (p+) regions were evaluated from dark J-V measurements. The laser process was applied to the stack composed of 50 nm Al_2O_3, 35 nm a-SiC_x (x~1), ~4 nm a-SiC_x(i) (x~0.1), 15 nm n-doped a-Si and 35 nm a-SiC_x (x~1) (Figure 4). Notice that, despite the intermediate n-doped a-Si included in such multilayer, punctual p++ regions could be formed after the laser step. This was a very remarkable result, as it allowed to simplify the fabrication process by eliminating one photolithographic step. Figure 4 shows the schematic of the sample for the testing laser process. The sample was irradiated using a pulsed Nd:YAG (Star-Mark SMP100 II Rofin-Baased) working at 1064 nm wavelength in TEM00 mode. The repetition frecuency was fixed at 4kHz with a laser pulse duration fixed of 100 ns. In our set-up, the laser power can be modified by adjusting the current of a pumping lamp. In particular, the quality of the laser-doped regions was explored in the power range from 800 mW to 1100 mW. The front surface of the sample was laser-processed to form a hexagonal matrix of spots separated a distance (pitch) of 300 µm. Each matrix corresponds to one device with a total area of 4.2 mm x 4.2 mm. Power conditions were varied between different devices to elucidate those that lead to higher quality junctions. The rear side was processed to create point contacts with 600 µm pitch to obtain an ohmic contact. After the laser processing steps, the sample was ready to be contacted and evaporated Ti/Al metallic stack.

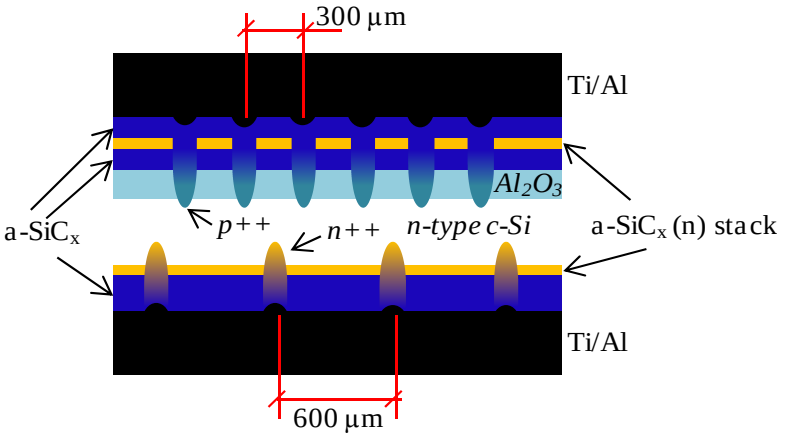

Fig. 4. p++/n diode scheme of the test samples fabricated for measuring the electrical behavior. Dark J-V curves were measured to identify optimal laser conditions

Figure 5a shows the sheet resistance as a function of the laser power measured with pour-point probe. For this measurement, a set of samples was specially prepared overlapping pulses to avoid any undoped area that could disrupt the current flow between the probes. Six areas of 1cm x 1 cm with different power laser conditions were irradiated. The result of these measurements should not be assumed as precise values of doping level, but can be used to compare the trend between different laser parameters and give us a power laser approximation. Figure 5b the dark J-V characteristics of the p++/n junctions created by laser doping. These measurements were done at 25 ºC and the current density was calculated dividing the measured current by the device area. A rectifying behaviour was observed in all the diodes irradiated from 810 mW to 1020 mW. The leakage current observed in the reverse biased region was also rather low. In all cases the dark J-V curves flatten at high fordward voltages. This behaviour due to ohmic losses in the series resistance typically hiders the exponential regions of the diode characteristic. The series resistance decreased as we increased the power of the laser in the range under evaluation. From 940 mW to 970 mW the diodes show better electrical behaviour considering both their series resistance and level of leakage current.

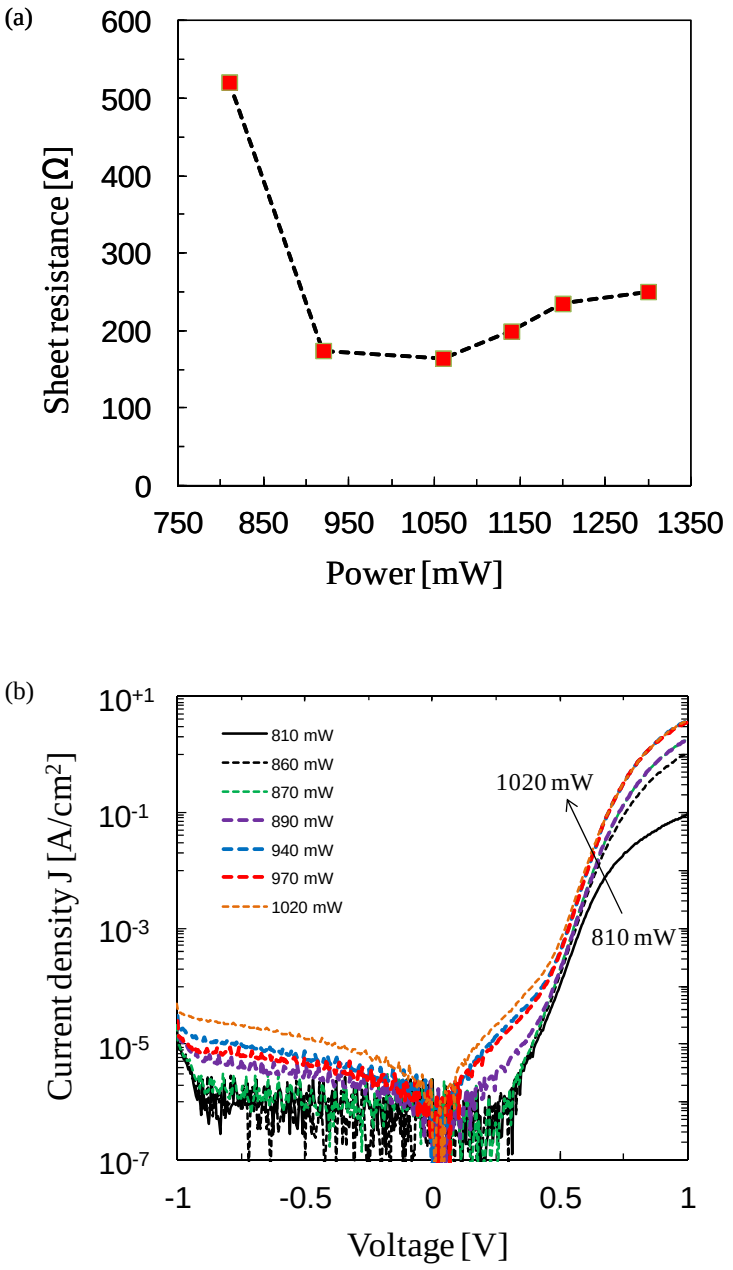

Fig. 5. (a) Sheet resistance measurements as a function of power laser. (b) Dark J-V measurements of diodes at different power laser conditions.

3.3. EQE and J-V measurements

Finally, four different emitter coverages (66%, 75%, 80% and 85%) with a pitch of 250 µm were irradiated to compare the influence of this parameter in the final device efficiency. Photovoltaic results of finished "cold" IBC solar cells are depicted in figure 6 and 6. From the EQE measurements (figure 6) we deduce that emitter coverage directly impacts the EQE. However, no clear trend can be deduced indicating a non-mature fabrication process that lead to different passivation qualities between samples. On the other hand, analysing the photovoltaic figures included in table 1, it is clear that fill factor (FF) is limiting the efficiency. Suns-V_{oc} measurements (figure 7) reveal that pseudo-fill factor (pFF) is 74.4% and consequently there is a FF loss of 9.3% abs. corresponding to series ohmic losses. These losses might be explained by laser power instability during the laser stage, resulting in a different laser spot morphology than expected. On the other hand, low V_{oc} values could be attributed to a certain surface passivation loss due to plasma etching resulting also in low EQE results. Nevertheless, an encouraging efficiency of 15.5% has been obtained in our first run of "cold" IBC solar cells. The improvement of the surface passivation after CF4 etching and the fine-tune of the power laser to the best value obtained in the dark J-V measurements are key to develop better devices in the future as our 3D simulations suggest (5).

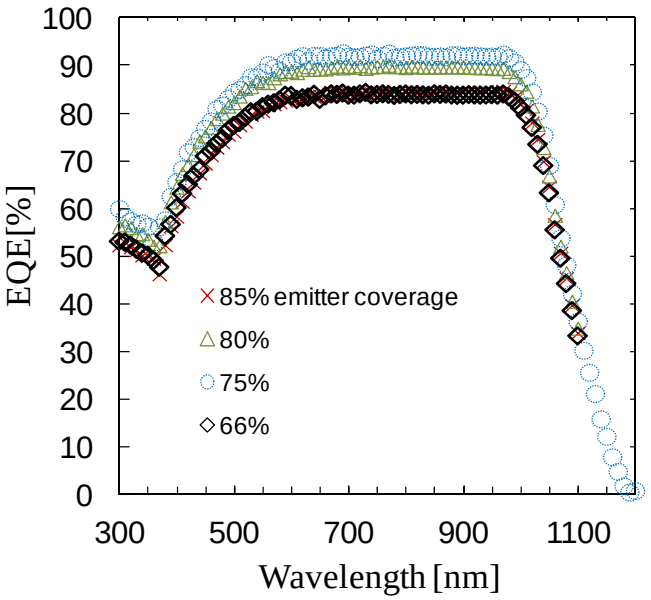

Fig. 6. EQE curves of the fabricated IBC solar cells, evaluating four different emitter coverages.

.

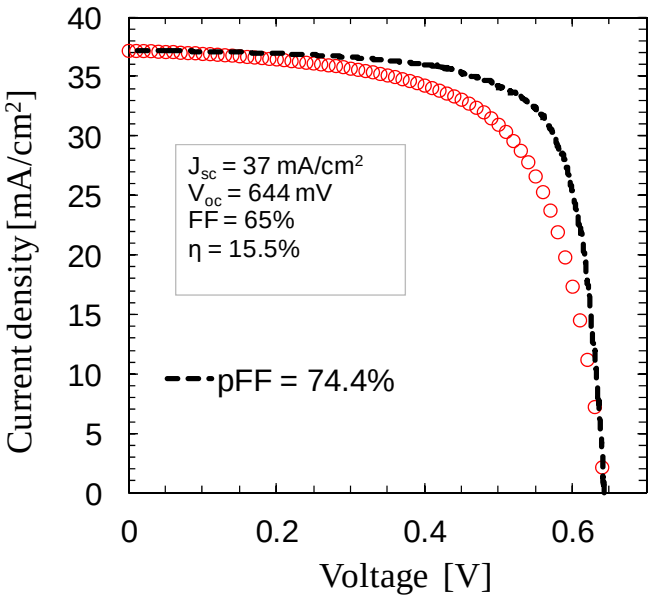

Fig. 7. Current density-voltage characteristics measured under AM1.5g illumination of the IBC with 75% emitter coverage. The dashed line corresponds to Suns-V_{oc} measurement.

Table 1. Photovoltaic parameters of four IBC with different emitter coverages

Emitter coverage [%]	V_{oc} (mV)	J_{sc} (mA/cm^2)	FF (%)	η (%)
85	623	34	57.3	12.1
80	620	36.4	65.4	14.7
75	644	37.2	65.1	15.5
66	635	33.7	60.1	12.7

4. Conclusions

Novel IBC solar cell structure has been proposed in a fully low-temperature fabrication process. Both the emitter and base contacts can be obtained in a single laser-processing step. Low-temperature deposited Al_2O_3 and a-SiC_x stacks deposited respectively by ALD and PECVD are the precursors of aluminum and phosphorous doping atoms, respectively. The fabrication process is simpler, as the photolithographic step to delimit emitter and base regions could be eliminated. Preliminary devices reached a promising 15.5% efficiency, mainly limited by the series resistance. Future work will focus on a fine tuning of the laser step, along with an optimization of etching steps to reduce the degradation of surface passivation.

Acknowledgements

This work has been supported by the Spanish Government under project TEC 2014-59736-R, ENE2013-48629-C4-1-R and by the European Union's Seventh Framework Programme for research, technological development and demonstration under project HERCULES (Grant agreement:608498).

References

[1] Kress A, Breitenstein O, Glunz S, Fath P, Willeke G, Bucher E. Investigations on low-cost back-contact silicon solar cells. Sol Energy Mater Sol Cells. Elsevier Science Publishers B.V.; 2001;65(1):555–60.
[2] Zin N, Blakers A, McIntosh KR, Franklin E, Kho T, Chern K, et al. Continued Development of All-Back-Contact Silicon Wafer Solar Cells at ANU. PV Asia Pacific Conference 2012. Energy Procedia; 2013 (33):50-63.
[3] Masuko K, Shigematsu M, Hashiguchi T, Fujishima D, Kai M, Yoshimura N, et al. Achievement of More Than 25% Conversion Efficiency With Crystalline Silicon Heterojunction Solar Cell. IEEE J Photovoltaics 2014;4(6):1433–5.
[4] Reichel C, Granek F, Hermle M, Glunz SW. Back-contacted back-junction n -type silicon solar cells featuring an insulating thin film for decoupling charge carrier collection and metallization geometry. Prog Photovoltaics Res Appl. 2013;21(March 2012):1063–76.
[5] Carrio D, Ortega P, Martín I, López G, López-González JM, Orpella A, Voz C and Alcubilla R. Rear contact pattern optimization on 3D simulations for IBC solar cells with point-like doped contacts. 4th Int Conf Silicon Photovoltaics, Silicon PV. 2014; Energy Procedia,55:47-52.
[6] Okanovic M, Jäger U, Ahrens M, Stute U. Influence of different laser parameters in laser doping from phosphosilicate glass. 24th EUPVSEC 2009, Hamburg (Germany).
[7] Werner JH, Röder TC, Eisele SJ, Grabitz P, Köhler JR. Laser Doped Selective Emitters Yield 0.5% Efficiency Gain. 24th EUPVSEC 2009, Hamburg (Germany).
[8] Colina M, Martín I, Voz C, Morales-Vilches A, Ortega P, López G, Orpella A, Alcubilla R, Sánchez-Aniorte I, Molpeceres C. Optimization of laser doping processes for the creation of p+ regions from solid dopant sources. 27 th EUPVSEC 2012. Frankfurt (Germany).
[9] Ogane A, Hirata K, Horiuchi K, Kitiyanan A, Uraoka Y, Fuyuki T. Feasible control of laser doping profiles in silicon solar cell processing using multiple excitation wavelengths. 2008 33rd IEEE Photovolt Spec Conf. 2008;
[10]Kray D, Fell A, Hopman S, Mayer K, Willeke G, and Glunz SW . Laser chemical processing (LCP). A versatile tool for microstructuring applications. Appl Phys A Mater Sci Process. 2008;93:99–103.
[11]Kray D, McIntosh KR. Analysis of Selective Phosphorous Laser Doping in High-Efficiency Solar Cells. IEEE Trans Electron Devices 2009;56(8):1645–50.
[12]Paviet-Salomon B, Gall S, Monna R, Manuel S, Slaoui A, Vandroux L, et al. Laser doping using phosphorus-doped silicon nitrides. Energy Procedia 2011;8:700–5.
[13]Suwito D, Jager U, Benick J, Janz S, Hermle M, Glunz SW. Industrially Feasible Rear Passivation and Contacting Scheme for High-Efficiency n-Type Solar Cells Yielding a V_{oc} of 700 mV. IEEE Trans Electron Devices 2010;57(8):2032–6.
[14]Fell A, Franklin E, Walter D, Suh D, Weber KJ. Laser Doping from Al_2O_3 layers. 27th EUPVSEC 2012. Frankfurt (Germany)
[15]Werner F, Veith B, Tiba V, Poodt P, Roozeboom F, Brendel R, et al. Very low surface recombination velocities on p- and n-type c-Si by ultrafast spatial atomic layer deposition of aluminum oxide. Appl Phys Lett; 2010;97(16):162103
[16]Martín I, Ortega P, Colina M, Orpella A, López G, Alcubilla R. Laser processing of Al_2O_3 /a-SiCx :H stacks: a feasible solution for the rear surface of high-efficiency p-type c-Si solar cells. Prog Photovoltaics Res Appl;2012;21(5):1171–5.
[17]Ortega P, Martín I, Lopez G, Colina M, Orpella A, Voz C, et al. p-type c-Si solar cells based on rear side laser processing of Al_2O_3/SiCx stacks. Solar Energy Materials and Solar Cells; 2012;106:80–3.
[18]Granek F. High-efficiency back-contact back-junction silicon solar cells 2009.